PREDICTION OF THE ULTIMATE STRENGTH OF REINFORCED CONCRETE BEAMS FRP-STRENGTHENED IN SHEAR USING NEURAL NETWORKS

R. Perera[a*], M. Barchín[a], A. Arteaga[b], A. De Diego[b]

[a] *Department of Structural Mechanics, Technical University of Madrid, José Gutiérrez Abascal 2, Madrid 28006, Spain*
[b] *Eduardo Torroja Institute for Construction Science, CSIC, Serrano Galvache 4, Madrid 28033 Spain*

Keywords: C. Computational modelling; CFRP materials; RC beams strengthening

Abstract

In the last years, a great number of experimental tests have been performed to determine the ultimate strength of reinforced concrete beams retrofitted in shear by means of externally bonded fibre reinforced polymers (FRP). Most of design proposals for shear strengthening are based on a regression analysis from experimental data corresponding to specific configurations which makes very difficult to capture the real interrelation among the involved parameters. To avoid this, an artificial neural network has been developed to predict the shear strength of concrete beams reinforced with this method from previous tests. Furthermore, a parametric study has been carried out to determine the influence of some beam and external reinforcement parameters on the shear strength with the purpose of reaching more reliable designs. Finally, some modifications of the design expressions are proposed and checked with experimental results.

1. Introduction

The use of fibre reinforced polymer (FRP) sheets as externally bonded reinforcement is nowadays widely recognized as an efficient method for strengthening and upgrading reinforced concrete (RC) members [1]. Carbon fibre-reinforced polymers (CFRP) have a high strength and stiffness-to-weight ratio, and show excellent fatigue behaviour and

* Corresponding author. Tel: +34 913363278. Fax: +34 913363004
E-mail address: perera@etsii.upm.es (R. Perera)

corrosion resistance. FRP plates may be prefabricated or constructed on site in a wet lay-up process.

Although FRPs have been widely used for column strengthening by external wrapping, flexural and shear FRP reinforcing elements, externally bonded to RC beams, constitute the larger body of current applications.

As a result of their growing application, some code proposals or recommendations [2-6] have been published in different countries or continents for the design of reinforced concrete (RC) structures reinforced or strengthened with FRP. Although some of these guidelines were published as early as the year 2000, and since then new knowledge has been developed and many topics are currently being investigated, they represent the state-of-the-art up to that date and therefore, except for some improvements, can be adopted as design guideline. The topics contained in these proposals cover design recommendations for the flexural strengthening of beams and slabs, the shear strengthening of beams and columns and the flexural and compressive strengthening of columns.

In these guidelines, flexural strengthening and confinement seem to be well understood although some obscure points still remain. However, the understanding of concrete structures designed for strengthening in shear is still an area where uniform design rules do not exist or are treated very briefly [7-16]. The cause of shear failure is a result of a complicated mechanism even for simple RC elements, so it would be even more complex when external FRP reinforcement is added to the concrete. Because of this, the prediction of the ultimate shear strength of reinforced concrete (RC) beams is critical especially when the value is used in the design and, therefore, a lot of theoretical and experimental work is still in progress to solve open questions.

In all existing design proposals, the design shear strength of an FRP-strengthened RC beam is evaluated from the contribution of concrete, the contribution of the steel stirrups and the contribution of the FRP. The first two contributions may be calculated according to the provisions in existing design codes, so the main differences among available proposals lie in the evaluation of the FRP contribution. Empirical [9, 12] and analytical equations [15-18] have been developed using regression analysis of experimental data.

To develop such models, the form of the empirical equation should be assumed and then the unknown parameters are determined. However, the great number of parameters that affect the beam strength makes the success of this procedure difficult.

By contrast, the use of artificial neural networks (ANN) provides an alternative method that overcomes these difficulties. An ANN is a computational tool that attempts to simulate the architecture and internal operational features of the human brain and neuron system. To perform this purpose, it consists on an interconnected network of processing elements that has the ability to be trained to map a given input into the desired output. Much of the success of neural networks is due to such characteristics as nonlinear processing, parallel processing and their ability to learn and generalize, i.e., producing reasonable outputs for inputs not encountered during training (learning). Neural network techniques have been successfully applied to different areas of structural engineering such as structural analysis and design [19, 20, 21], damage assessment [22, 23] and constitutive modelling [24].

The intended aim of this study is to explore the feasibility of using a multilayer feed-forward artificial neural network to predict the ultimate shear strength of RC beams shear strengthened with FRP composites. For this purpose, a database of 61 RC beams was retrieved from existing literature for analysis. Results obtained are compared with

some experimental values and with those determined from some design guidelines [2, 3, 4, 5] and proposals [16] to assess the performance of the neural network in predicting the shear capacity of the strengthened beams.

The presentation of this work is organized as follow. Some existing design proposals are first briefly reviewed. The NN is then developed, and the trained NN is validated against experimental data collected from the existing literature. Some parametric studies will contribute to a better understanding of the influence of various parameters on the shear capacity of the strengthened beam and, finally, based on these studies, some modifications of the design equations are proposed.

2. Existing design proposals

Common methods of shear strengthening include side bonding, U-jacketing and wrapping (Fig.1). Both FRP strips and continuous sheets have been used. Furthermore, the fibres in the FRP may also be orientated at different angles. Therefore, different strengthening schemes are possible which will influence the failure mode.

Several design guidelines and proposals [11, 12, 18] have been proposed in recent years for the prediction of the shear strength of RC beams when shear strengthened with FRP. In all existing design proposals, the design shear strength, V_d, of an FRP-strengthened RC beam is evaluated from

$$V_d = V_c + V_s + V_f \tag{1}$$

where V_c is the contribution of concrete, V_s is the contribution of the steel stirrups and V_f is the contribution of the FRP. V_c and V_s may be calculated according to the provisions in existing design codes, so the main differences among available proposals lie in the evaluation of the FRP contribution V_f.

Some of the proposals, which are selected and used in this study for comparison with the results from the neural networks, are outlined in the following.

2.1. fib Bulletin 14 [2]

Strengthening guidelines have been put together by a European task group presented in a technical report drawn up in accordance with the design format of Eurocode 2 [25]. The group consists of about 60 members representing most European universities, research institutes and industrial companies working in the field of advanced composite reinforcement for concrete structures. In this proposal, the FRP contribution to shear capacity is determined by analogy to the internal steel, according to the model of Triantafillou [9] and Täljsten [26], and is as follows:

$$V_f = 0.9\varepsilon_{fd,e} E_f \rho_f b_w d(\cot\alpha + \cot\beta)\sin\beta \qquad (2)$$

where (Fig. 2):

$\varepsilon_{fd,e}$= design value of effective FRP strain

d= effective depth of cross section

b_w= minimum width of cross section over the effective depth

ρ_f= FRP reinforcement ratio equal to $2t_f \text{sen}\alpha/b_w$ for continuously bonded shear reinforcement and $2(t_f/b_w)(w_f/s_f)$ for strips or sheets of width b_f at a spacing s_f

t_f= thickness of the FRP transversal reinforcement

s_f= spacing of the FRP transversal reinforcement

w_f= breadth of the FRP transversal reinforcement

E_f= elastic modulus of FRP in the principal fibre orientation

α= angle of diagonal crack with respect to the member axis

β= angle between the principal fibre orientation and the longitudinal axis of the member

The design value of effective FRP strain is obtained from a regression analysis on experimental results of RC members shear strengthened with different FRP bonding configurations [2].

2.2. ACI 440.2R-02 [3]

In this proposal, prepared by the American Concrete Institute, the shear contribution of the FRP shear reinforcement is given by:

$$V_f = \frac{2nt_f w_f E_f \varepsilon_{fd,e} \left(\cos\beta + sen\beta\right) d_f}{s_f} \tag{3}$$

where n is the number of plies of FRP reinforcement.

In this proposal, the FRP effective strain is limited to 0.4% for completely wrapped members while for bonded U-wraps or bonded face plies it is calculated using a bond-reduction coefficient κ_v

$$\varepsilon_{fd,e} = \kappa_v \varepsilon_{fu} \leq 0.004 \tag{4}$$

where ε_{fu} is the design rupture strain of FRP reinforcement. The bond-reduction coefficient is computed as follows [11]:

$$\kappa_v = \frac{k_1 k_2 L_e}{11900\varepsilon_{fu}} \tag{5}$$

where L_e is the length over which the majority of the bond stress is maintained and k_1 and k_2 are two coefficients accounting for the concrete strength and the type of wrapping scheme used [3].

2.3. Technical Report 55 – Concrete Society [4]

In this report, originally published in December 2000 by the UK Concrete Society, the contribution of the FRP to the shear capacity is given by:

$$V_f = E_{fd}\varepsilon_{fd,e}A_f\frac{\left(d_f - \frac{n}{3}l_{t,\max}\right)}{s_f}\left(\cos\beta + sen\beta\right) \quad (6)$$

where:

n = 0 for a fully wrapped beam, 1 for U jacketing and 2 for side bonding.

A_f = area of FRP (mm^2) for shear strengthening measured perpendicular to the direction of the fibres.

d_f = effective depth of the FRP strengthening, measured from the top of the FRP to the tension reinforcement (mm) (Fig. 2).

E_{fd} = elastic modulus of FRP in the principal fibre orientation

$l_{t,max}$ = anchorage length required to develop full anchorage capacity

$$l_{t,\max} = 0.7\sqrt{\frac{E_{fd}t_f}{f_{ctm}}} \quad (7)$$

where f_{ctm} is the tensile strength of the concrete (N/mm^2)

The effective strain in the FRP is taken as the minimum of:

- $\varepsilon_{fd}/2$ (8)
- $0.64\sqrt{\frac{f_{ctm}}{E_{fd}t_f}}$ (9)
- 0.004 (10)

where ε_{fd} is the design ultimate strain capacity of FRP.

The three expressions used to calculate the effective strain correspond to different design models [27-30].

2.4. CNR-DT 200/2004 [5]

This technical document was published by the Italian Research Council in 2004. In the same way as the European guidelines [2] the design proposals vary with reinforcement configurations:

- Rectangular cross section and FRP side bonding configuration

$$V_f = \frac{1}{\gamma_d} \min\{0.9d,\ h_f\} f_{fd,e} 2t_f \frac{sen\beta}{sen\alpha} \frac{w_f}{p_f} \tag{11}$$

- Rectangular cross section and U-wrapped or completely wrapped configurations

$$V_f = \frac{1}{\gamma_d} 0.9df_{fd,e} 2t_f \left(\cot\alpha + \cot\beta\right) \frac{w_f}{p_f} \tag{12}$$

where $f_{fd,e}$ is the effective FRP design strength, γ_d is a factor assumed equal to 1.2, p_f is the FRP spacing measured in the same direction of w_f and h_f is the height of the FRP reinforcement (Fig. 2).

As in previous cases, different expressions are given for $f_{fd,e}$ depending on the FRP reinforcement configuration.

2.5. Cheng and Teng's model [16]

This model was derived by assuming that discrete FRP strips can be modelled as an equivalent continuous FRP sheet/plate and its contribution is given by

$$V_f = 2f_{f,e} t_f b_f \frac{h_{fe}\left(\cot\alpha + \cot\beta\right)\sin\beta}{s_f} \tag{13}$$

where f_{fe} is the average stress of the FRP intersected by the shear crack at ultimate limit state and h_{fe} is the effective height of the FRP bonded on the web (Fig.3).

This model assumes that the stress distribution in the FRP along a shear crack is non-uniform at the ultimate limit state and, therefore, an average stress is calculated as follows:

$$f_{f,e} = D_f \sigma_{f,\max} \tag{14}$$

in which $\sigma_{f,\max}$ is the maximum stress that can be reached in the FRP intersected by the shear crack and D_f is a stress distribution factor. The values of both parameters depend on whether the shear failure is controlled by FRP rupture or FRP debonding [27].

3. Neural network-based modelling of shear strength of strengthened RC beams with FRP

3.1. Fundamental aspects of neural networks

Neural networks are a useful tool for information processing and many other applications. Due to their unique features they can be used to solve complex problems that cannot be handled by analytical approaches, even problems whose underlining physical and mathematical models are not well-known. From this point of view, they might be suitable for determining the shear capacity of RC beams strengthened with FRP shear reinforcement.

Artificial neural networks consist of a number of processing units or neurons interacting with each other via weighted connections to constitute a network and are characterized by an architecture or topology and a learning mechanism. The processing units may be grouped into layers of input, hidden and output neurons. The interconnection topology defines the number of the types of arrangements. The topology of a three-layer feedforward is presented schematically in Fig. 4; nodes represent the neurons and the arcs the connections. The NN in the figure consists of five input neurons, seven hidden

neurons and three output neurons. The number of input and output neurons depends on the problem to be solved while the number of hidden layers and the neurons per layer may be determined by checking different configurations until the optimum is reached. Learning is achieved by updating the weights associated with the links among neurons based on known input and output patterns or training patterns using an iterative procedure. These weights represent the strength of the connections among the neurons. The remarkable computational characteristics of neural networks are their ability to learn functional relationships from training examples and to discover patterns and regularities in variables by simply presenting them with data. Among the available training methods, back-propagation is the most successful and widely used. By applying this method, once the input is propagated from the input layer through the hidden layers to the output layer, the error between the predicted and expected output values is then back-propagated from the output to the input layer modifying the connection weights. The process is repeated until the error is minimized.

3.2. Neural network modelling

For the configuration and learning of the NN, 61 experimental tests of nine authors [referencias] were considered in detail, collecting the database reported in Appendix A. The database includes beams shear strengthened with FRP using different configurations. Furthermore, the selected tests present a high diversity regarding the beam geometric ratios, reinforcement ratios, material properties and, therefore, failure loads.

The resisting shear mechanisms differ depending on the FRP reinforcement configuration. In fact, it is usually assumed that in the case of U-jacketing and wrapping

the resisting mechanism is based on the Moersch truss, while in the case of side bonding, because the Moersch truss cannot form as the tensile diagonal tie is missing, a different resisting mechanism is assumed based on crack-bridging [31]. For this reason, the study was restricted to U-jacketing and wrapping beams and, therefore, 15 beams were removed to ensure a satisfactory generalization in the network.

The beam parameters available from the experimental database are the geometry of the beam, the mechanical properties and configuration of concrete and internal reinforcement, and the geometry, configuration and mechanical properties of the external reinforcement. Taking into account the high number of parameters which influence the shear failure mode, a suitable selection of the input variables is essential to reach an optimum configuration of the NN. Furthermore, the number of input parameters should also be chosen according to the number of training data. With a training set of less than 100 data it is not convenient to use more than 8 or 10 input variables.

The way of choosing the input parameters representing the characteristics of the problem studied is one of the most important points to ensure the success of this approach. On the one hand, the number of parameters must be large enough to represent the system properly. However, on the other hand, a large number of input neurons in the NN may reduce the efficiency and accuracy of the training process. In this case, the choice of the input parameters has been guided based on the shear capacity equations, summarized previously, of the different design proposals. For this reason, the theoretical shear capacity of the experimental beams collected in Appendix A has been calculated with the five design proposals. In accordance with the different proposals, the following design rules were used, to calculate the contribution of concrete and steel

stirrups in Eq. (1): a) Eurocode2: Part 1 [25]; b) EHE-Concrete Spanish code [32]; b) BS 8110 : Part 1 [33]; c) ACI 318-02 [34].

By suitably combining the different design guidelines for strengthening using FRP with the different codes for concrete, eight theoretical predictions were obtained. In Table 1 the comparison between predicted values and experimental values for the data used in the NN is shown. To perform this comparison in a suitable way, it is necessary to take into account that the safety factors involved in the different guidelines are included in the theoretical predictions.

From the results, it is clear that the best predictions were obtained when the design guidelines contained in fib Bulletin 14 were used. Although this does not allow concluding that this guide is the most suitable for FRP strengthening design, fib Bulletin 14, EHE and Eurocode 2 were taken as a basis for selecting the input parameters to the NN. After the study, the nine major variables selected are listed as follows:

- breadth of the beam (b_w; mm)
- height of the beam section (h; mm)
- ratio of the FRP transversal reinforcement (ρ_f)
- angle between the principal fibre orientation and the longitudinal axis of the member (β)
- elastic modulus of the FRP reinforcement (E_f; MPa)
- ratio of the longitudinal steel reinforcement (ρ_l)
- cross sectional area of transverse steel per length unit (A_{90}; mm^2/mm)
- design yielding stress of the shear steel reinforcement ($f_{y90,d}$)
- characteristic compression strength of the concrete (f_{ck}; MPa)

Therefore, the NN will be configured with nine input neurons and one output neuron which represents the value of the shear strength of the RC beam shear strengthened with FRP.

3.3. Training

Once some test beams were removed, 46 beams were used to train and test the artificial neural network. The 46 test beams were grouped randomly into two sets: a training set containing 38 beams, and a validating set with 8 beams. To avoid the slow rate of learning near the end points the input and output data were scaled between the interval [-1, 1].

After a number of trials, the values of the network parameters considered by this study were as follows:

- Number of input parameters: 9
- Number of output parameters: 1
- Number of hidden layers: 1
- Number of hidden neurons: 11
- Hyperbolic tangent activation function in the first layer and in the hidden layer
- Identity activation function in the last layer
- Back-propagation training algorithm with momentum
- Momentum factor: 0.9
- Learn rate: 0.15
- Training cycles: 3000

$$\delta = \frac{1}{n}\sum_{i=1}^{n}(t_i - x_i)^2 \qquad (15)$$

where t_i are the experimental values and x_i the values predicted by the network. The value of this error is 0.0061 for the validation set and 0.0039 for the total experimental set (training + validation).

In addition, the ratio between the experimental and predicted shear strengths has been calculated for the validation set resulting in a mean value of 1.0496 with a variance of 16.35 %. Maximum and minimum values for this ratio were 0.8455 and 1.3488, respectively.

All the previous results indicate that the error has been reduced to an acceptable level and the network learning can be qualified as correct although the possibility of obtaining better results with another configuration cannot be discarded.

3.4. Comparison with experimental results

Figs. 5a and 5b show the predictions of the NN as compared to the experimental values for both training and test data. The predictions lie above and below the target line, i.e., the line where the predicted value is equal to the experimental value. The nearer the points gather around the diagonal line, the better the predicted values. As was to be expected better predictions are obtained for the training set although in both cases, the low scatter of data around the diagonal line confirms the efficiency of the NN as predictor of the shear stress capacity. From a comparison point of view, the linear regression slope and the linear correlation coefficient for the training data are 0.957 and 0.9801, respectively, while for the validation data these values are 1.04 and 0.9841.

3.5. Comparison with design proposal predictions

The neural network predictions were also compared with the predictions of the design equations summarized in Section 2. Table 2 presents the comparison of the predictions of the neural network model with the different design models and the experimental results for the validation data taken from Appendix A. With the same purpose, Table 3 shows the mean percentage errors for the total set of data and for the validation data. As is logical, the error in the NN predictions is clearly lower than the errors using the design proposals since, in the first case, none safety partial factor was considered. Therefore, the design equations give more conservative predictions. However, the neural network model might be used for design and verification of the shear behaviour of RC beams strengthened with FRP by applying an appropriate safety factor to the predicted value. The more the amount of experimental data used to train the NN, the fitter the value of the safety factor since the neural network model will improve.

4. Parametric studies based on the ANN

After the network has been adequately trained, it is possible to generate new beams to make it easy to study the influence of the different parameters which affect the failure shear strength by simply varying one input parameter and keeping the others constant. Furthermore, through parametric studies, the performance of the NN in simulating the physical behaviour of the shear strengthening of an RC beam can be verified. Neural network predictions consistent with the experimental tests yield a qualitative evidence of the ability of the NN to simulate the physical phenomenon.

Furthermore, taking into account the diversity of empirical equations proposed in the different design proposals, the parametric analysis can be useful as a basis for determining the most influential parameters in the problem under study with the

purpose of proposing future modifications to the empirical equations. To do this, the NN predictions have been compared with the theoretical predictions of the different design guidelines summarized in Section 2. The contribution of concrete and steel stirrups was calculated with the corresponding concrete codes as in Section 3.2. Figs. 8a-d plot the failure shear strength of a series of RC beams externally reinforced with shear FRP as a function of b_w, A_{90}, t_f and β as indicated in the graphs.

From Figs. 6 it is evident that the network has apparently learned the behaviour of RC beams strengthened with FRP. For the cross sectional area of transverse steel per length unit (A_{90}) and for the FRP thickness (Figs 6b and c) the agreement between the NN predictions and the design guidelines predictions is sufficiently satisfactory since the curves follow a similar tendency although the most conservative values are always obtained with Cheng and Teng's equation [16]. However, according to Fig.6d , the effect of the angle between the principal fibre orientation and the longitudinal axis of the member, β, is not suitably considered in the design equations since its influence should be higher. In any case, more experimental results for training the network would be necessary to confirm this fact. In the same way, according to the NN predictions, the beam width effect (b_w) over the shear capacity would be under-estimated from a certain value.

To identify the most important parameters to estimate the shear capacity according to the neural network, the Garson index has been used [35]. Through operations between the weight matrices generated in two consecutive layers of the NN, the Garson index identifies the relative importance of all input variables regarding the output variable. For an NN with one hidden layer the Garson index is defined as follows:

$$G_{ik} = \frac{\sum_{j=1}^{J} \frac{|W_{ij}||V_{ik}|}{\sum_{i=1}^{I}|W_{ij}|}}{\sum_{i=1}^{I}\sum_{j=1}^{J} \frac{|W_{ij}||V_{jk}|}{\sum_{i=1}^{I}|W_{ij}|}} \quad (17)$$

where G_{ik} is the relative importance, measured in so much per one, assigned between the ith parameter of the input layer and the kth prediction of the output layer; $[W_{ij}]$ is the weight matrix linking the I neurons of the input layer with the J neurons of the intermediate hidden layer and $[V_{ij}]$ is the weight matrix linking the J neurons of the hidden layer with the K neurons of the output layer.

Table 4 shows the Garson index for the nine input parameters considered in the final NN configuration. It is clear that the highest relative importance is assigned to the ratio of the FRP transversal reinforcement (ρ_f) although parameters like the cross sectional area of transverse steel per length unit (A_{90}) and the angle between the principal fibre orientation and the longitudinal axis of the member (β) also have an important weight. However, there are parameters whose relative importance is low such as the beam geometry and the characteristic compression strength of the concrete (f_{ck})

5. Possible approaches for a new shear design equation

One of the purposes of the present study is the proposal of modifications to the design equations used to calculate the contribution of the external reinforcement in Eq.(1) from the NN predictions.

To perform this, the experimental tests performed by Monti and Liotta [31] have been taken as a reference since the FRP contribution is known in them. Table 5 shows the experimental values as well as the predictions with the different equations summarized

in Section 2. Predictions performed with the fib Bulletin 14 are clearly higher than the experimental values. This feature is similar for the other design model proposals except for Cheng and Teng´s model [16]. However, the predictions on the total shear capacity are conservative when a suitable code is adopted to estimate the contributions of concrete and steel. Therefore, modifications should be performed on the design equations which calculate the contribution of the FRP reinforcement with the purpose of obtaining more conservative predictions. Since, according to Table 1, better predictions were obtained when the fib Bulletin 14 combined with Eurocode 2 and EHE was applied, the proposed modifications are performed on Eq.(2).

From the parametric analysis performed in the previous section, it was demonstrated that the angle between the principal fibre orientation and the longitudinal axis of the member, β, predicted by the NN has a greater influence when compared with the equations of the current design guidelines. This should be reflected in any proposed modification. Furthermore, fib 14, unlike other guidelines, does not take into account the effect of the effective depth of the FRP strengthening (d_f in Fig.2) which it might be convenient to include. Therefore, the proposed modifications in this study have been orientated towards these two parameters, β and d_f, although other approaches might be also considered.

To introduce the effect of d_f in Eq.(2), a similar approach to that used to evaluate the FRP reinforcement ratio has been considered by the introduction of a new factor in Eq.(2), defined as follows:

$$k_d = \frac{d_f}{d} \tag{18}$$

On the other hand, in order to adapt Eq. (2) to take into account the higher influence of the angle β, a new factor, k_β, has been included to reflect that the optimum orientation of the fibres corresponds to 45º. From Fig.6d, the total shear capacity can decrease

approximately by 60% from a configuration of 45º to another of 90º. Then, as firstly the maximum value has been assumed to be reached when β=45º, it is assumed, secondly, that the coefficient k_β takes on a value of 0.4 when β=90º, i.e., 40% of the maximum contribution. On the other hand, finally, from a safety point of view, the maximum value of this coefficient has been assumed to be equal to 0.8 when β=45º. With these three conditions the expression for k_β is as follows:

$$k_\beta(\beta) = -1,97 \times 10^{-4} \beta^2 + 0,0177\beta + 0,4 \quad (19)$$

where β is the angle in degrees.

With the modifications proposed in Eqs.(18) and (19), Eq. (2) has been applied again to evaluate the contribution of FRP in the experimental tests shown in Table 5. Predicted values and comparison with experimental values are shown in Table 6. As may be observed, the agreement of the predictions with the experimental tests is satisfactory and for almost all the specimens the estimations are conservative. Therefore, the proposed modifications represent an improvement in terms of estimation of the FRP contribution over all the other design guidelines. However, this study represents a first step and, in order to confirm the proposed modifications and propose new ones, new studies should be performed considering a wider experimental database.

6. Conclusions

A study related to the strength of RC beams strengthened with FRP in shear has been performed. To do this, an artificial neural network has been developed to predict this shear strength using a database of experimental results. With the neural network predictions, a comparative study has been carried out with the experimental results and

with the predictions of other design proposals showing the high accuracy of the strength values obtained from the artificial neural network.

With the NN model some parametric studies have been also carried out and the Garson index has been calculated for the input parameters to the NN with the purpose of identifying the most important parameters to estimate the shear capacity. A high influence has been assigned to the ratio of the FRP transversal reinforcement, the cross sectional area of transverse steel and the angle between the principal fibre orientation and the longitudinal axis of the member while parameters such as the beam geometry and the characteristic compression strength of the concrete have a lower relative importance.

Based on the parametric study, modifications in the design equations have been developed which should be confirmed in the future with new experimental data.

Although the present NN model successfully simulates the desired phenomenon there is still need to improve the accuracy of the predictions by increasing the training database. Only when a sufficient number of data is considered will the NN be able to model in an accurate way the complex mechanisms of interaction among the multiple variables. However, the study has shown the potential of NNs to predict the shear strength of externally strengthened beams and should constitute a first step for future developments.

Acknowledgements

The writers acknowledge support for the work reported in this paper from the Ministry of Education and Science of Spain (project BIA2007-67790) and the Ministry of Public Works (project 80010/A04)

Table A.1. Geometrical and mechanical data of the experimental RC beams

Author	Index	Geometrical parameters				Mechanical characteristics and configuration						
						Concrete		Steel				
		h (mm)	h_w (mm)	b_w (mm)	c (mm)	f_{ck} (MPa)	f_{ctm} (MPa)	$f_{y90,d}$ (MPa)	A_c	s_c	A_{90}	A_t
Monti [31]	US60	450	300	250	30	3,2	0,7	347,8	100,5	400,0	0,25	1256,0
	USVA	450	300	250	30	3,2	0,7	347,8	100,5	400,0	0,25	1256,0
	USV+	450	300	250	30	3,2	0,7	347,8	100,5	400,0	0,25	1256,0
	US45+	450	300	250	30	3,2	0,7	347,8	100,5	400,0	0,25	1256,0
	UF90	450	300	250	30	3,2	0,7	347,8	100,5	400,0	0,25	1256,0
	US45++	450	300	250	30	3,2	0,7	347,8	100,5	400,0	0,25	1256,0
	WS45++	450	300	250	30	3,2	0,7	347,8	100,5	400,0	0,25	1256,0
	US45+ "A"	450	300	250	30	3,2	0,7	347,8	100,5	400,0	0,25	1256,0
	US45++ "B"	450	300	250	30	3,2	0,7	347,8	100,5	400,0	0,25	1256,0
	US45++ "C"	450	300	250	30	3,2	0,7	347,8	100,5	400,0	0,25	1256,0
	US45++ "F"	450	300	250	30	3,2	0,7	347,8	100,5	400,0	0,25	1256,0
	US45++ "E"	450	300	250	30	3,2	0,7	347,8	100,5	400,0	0,25	1256,0
	US45+ "D"	450	300	250	30	3,2	0,7	347,8	100,5	400,0	0,25	1256,0
Khalifa Nanni [13]	BT2	405	405	150	34	27,0	2,7	434,8	0,0	-	0,00	1230,9
	BT4	405	405	150	34	28,0	2,8	434,8	0,0	-	0,00	1230,9
Kamiharako [36]	2	500	500	250	100	24,6	2,5	453,0	0,0	-	0,00	2267,1
	3	500	500	250	100	24,6	2,5	453,0	0,0	-	0,00	2267,1
	7	500	500	250	100	26,6	2,7	453,0	0,0	-	0,00	3400,6
	8	500	500	250	100	26,6	2,7	453,0	0,0	-	0,00	3400,6
Umezu [37]	AS1	300	300	150	28	35,0	3,2	365,2	0,0	-	0,00	441,6
	AS2	300	300	150	28	35,0	3,2	365,2	0,0	-	0,00	441,6
	AS3	300	300	150	28	36,8	3,3	365,2	0,0	-	0,00	441,6
	CS1	300	300	300	43	32,5	3,1	365,2	0,0	-	0,00	883,1
	CS2	300	300	300	43	32,5	3,1	365,2	0,0	-	0,00	883,1
	CS3	300	300	150	43	36,8	3,3	365,2	0,0	-	0,00	441,6
	AB1	300	300	150	47	33,9	3,1	365,2	0,0	-	0,00	830,5
	AB2	300	300	300	47	37,6	3,4	365,2	0,0	-	0,00	1661,1
	AB3	300	300	300	47	33,9	3,1	365,2	0,0	-	0,00	1661,1
	AB4	300	300	300	47	33,9	3,1	365,2	0,0	-	0,00	1661,1
	AB5	300	300	300	47	34,7	3,2	365,2	0,0	-	0,00	1661,1
	AB8	300	300	600	47	35,5	3,2	365,2	0,0	-	0,00	3322,1
	AB9	450	450	450	51	31,9	3,0	365,2	0,0	-	0,00	4019,2
	AB10	550	550	550	51	31,9	3,0	365,2	0,0	-	0,00	5626,9
	AB11	550	550	550	51	32,6	3,1	365,2	0,0	-	0,00	5626,9
Funakawa [38]	S2	600	600	600	90	22,0	2,4	295,7	157,0	190,0	0,83	11253,8
	S3	600	600	600	90	22,0	2,4	295,7	157,0	190,0	0,83	11253,8
	S4	600	600	600	90	22,0	2,4	295,7	157,0	190,0	0,83	11253,8
Taerwe [39]	BS2	450	450	200	55	27,1	2,7	486,1	56,5	400,0	0,14	1884,0
	BS4	450	450	200	55	28,8	2,8	486,1	56,5	400,0	0,14	1884,0
	BS6	450	450	200	55	27,8	2,8	486,1	56,5	400,0	0,14	1884,0
Norris [40]	E	200	200	125	30	28,0	2,8	365,2	56,5	200,0	0,28	401,9
Chajes [8]	A	190	190	64	37	38,0	3,4	460,9	0,0	-	0,00	201,0
	E	190	190	64	37	38,0	3,4	460,9	0,0	-	0,00	201,0
	G	190	190	64	37	38,0	3,4	460,9	0,0	-	0,00	201,0
Park [41]	3	250	250	100	65	17,4	2,0	347,8	0,0	-	0,00	398,0
	6	300	300	100	65	17,4	2,0	347,8	0,0	-	0,00	663,3

Table A.2. Geometrical and mechanical characteristics of the FRP reinforcement and total shear capacity of the experimental strengthened RC beams

Author	Index	FRP characteristics and configuration						Total strength
		E_f (MPa)	f_{fd} (MPa)	w_f (mm)	t_f (mm)	p_f (mm)	FRP configuration	V_{tot} (kN)
Monti [31]	US60	390000	3000	150	0,22	300	U	111,0
	USVA	390000	3000	150	0,22	283	U	120,0
	USV+	390000	3000	150	0,22	283	U	135,0
	US45+	390000	3000	150	0,22	300	U	125,5
	UF90	390000	3000	150	0,22	300	U	125,0
	US45++	390000	3000	50	0,22	106	U	133,5
	WS45++	390000	3000	50	0,22	106	W	158,5
	US45+ "A"	390000	3000	150	0,22	159	U	167,0
	US45++ "B"	390000	3000	150	0,22	159	U	172,0
	US45++ "C"	390000	3000	150	0,22	159	U	182,9
	US45++ "F"	390000	3000	150	0,22	212	U	150,2
	US45++ "E"	390000	3000	150	0,22	212	U	163,5
	US45+ "D"	390000	3000	150	0,22	212	U	103,8
Khalifa Nanni [13]	BT2	228000	3800	167	0,165	334	U	156,0
	BT4	228000	3800	50	0,165	125	U	162,0
Kamiharako [36]	2	244000	3990	40	0,11	100	W	209,0
	3	90000	2920	40	0,169	100	W	218,6
	7	244000	3990	64	0,11	100	W	234,9
	8	90000	2920	64	0,169	100	W	232,3
Umezu [37]	AS1	73000	2700	200	0,044	245	W	91,2
	AS2	73000	2700	100	0,044	200	W	89,7
	AS3	73000	2700	200	0,088	245	W	114,0
	CS1	244000	4200	200	0,111	231	W	214,0
	CS2	244000	4200	100	0,111	200	W	159,0
	CS3	244000	4200	100	0,111	200	W	116,0
	AB1	73000	2700	200	0,044	228	W	110,0
	AB2	73000	2700	200	0,044	228	W	173,0
	AB3	73000	2700	200	0,088	228	W	209,0
	AB4	73000	2700	200	0,088	228	W	224,0
	AB5	73000	2700	200	0,144	228	W	254,0
	AB8	73000	2700	200	0,144	228	W	424,0
	AB9	73000	2700	200	0,144	359	W	379,0
	AB10	73000	2700	200	0,144	449	W	569,0
	AB11	73000	2700	200	0,288	449	W	662,0
Funakawa [38]	S2	240000	3800	200	0,167	459	W	691,0
	S3	240000	3800	200	0,334	459	W	795,0
	S4	240000	3800	200	0,501	459	W	942,0
Taerwe [39]	BS2	240000	3400	100	0,11	400	U	247,5
	BS4	240000	3400	50	0,11	400	U	170,0
	BS6	240000	3400	50	0,11	600	U	166,6
Norris [40]	E	34000	390	200	1	153	U	68,0
Chajes [8]	A	11000	200	200	1	138	U	34,4
	E	14000	170	200	0,46	138	U	35,4
	G	21000	185	200	0,58	138	U	37,0
Park [41]	3	155000	2400	25	1,2	75	U	44,0

6	155000	2400	25	1,2	75	U	53,6

U: U-jacketing; W: Wrapping

References

[1] Bank LC. Composites for construction: Structural design with FRP materials, John Wiley and Sons, 2006

[2] fib bulletin 14. Externally bonded FRP reinforcement for RC structures. Design and use of externally bonded fibre reinforced polymer reinforcement (FRP EBR) for reinforced concrete structures. Task group 9.3. FRP reinforcement for concrete structures. Lausanne, Switzerland, 2001.

[3] ACI 440.2R-02. Guide for the design and construction of externally bonded FRP systems for strengthening concrete structures. Reported by ACI Committee 440. American Concrete Institute, Farmington Hills, Michigan, USA, 2002.

[4] Concrete Society Technical Report 55. Design guidance for strengthening concrete structures using fibre composite materials. The Concrete Society, Crowthorne, 2000.

[5] CNR-DT200/2004. Guide for the design and construction of externally bonded FRP systems for strengthening existing structures. Italian National Research Council, Rome, Italy, 2004.

[6] Design Manual No.4. Strengthening reinforced concrete structures with externally-bonded fibre reinforced polymers. Isis Canada, The Canadian Network of Centres of Excellence on Intelligent Sensing for Innovative Structures, 2001.

[7] Al-Sulaimani GJ, Sharif AM, Basunbul IA, Baluch MH, Ghaleb BN. Shear repair for reinforced concrete by fibreglass plate bonding. ACI Struct J 1994; 91(3): 458-464.

[8] Chajes MJ, Januszka TF, Mertz DR, Thomson TA, Finch WW. Shear strengthening of reinforced concrete beams using externally applied composite fabrics. ACI Struct J 1995;92(3): 295-303.

[9] Triantafillou TC. Shear strengthening of reinforced concrete beams using epoxy-bonded FRP composites. ACI Struct J 1998; 95(2): 107-115.

[10] Triantafillou TC. Composites: a new possibility for the shear strengthening of concrete, masonry and wood. Compos Sci Technol 1998; 58 (8): 1285-1295.

[11] Khalifa A, Gold WJ, Nanni A, Aziz A. Contribution of externally bonded FRP to shear capacity of RC flexural members. J Compos Constr 1998; 2(4): 195-203.

[12] Triantafillou TC, Antonopoulos CP. Design of concrete flexural members strengthened in shear with FRP. J Compos Constr 2000; 4(4): 198-205.

[13] Khalifa A, Nanni A. Improving shear capacity of existing RC T-section beams using CFRP composites. Cement Concrete Compos 2000; 22: 165-174.

[14] Täljsten B, Elfgren L. Strengthening concrete beams for shear using CFRP-materials: evaluation of different application methods. Compos Part B-Eng 2000; 31(2): 87-96.

[15] Täljsten B. Strengthening concrete beams for shear with CFRP sheets. Constr Build Mater 2003; 17: 15-26.

[16] Chen JF, Teng JG, Smith ST, Lam L. FRP strengthened RC structures. John Wiley & Sons, 2001.

[17] Drimoussis A, Cheng JJR. Shear strengthening of concrete bridge girders using carbon fibre-reinforced plastic sheets. Fourth International Bridge Engineering Conference, San Francisco 1995: 337-347.

[18] Chaallal O, Nollet MJ, Perraton D. Strengthening of reinforced concrete beams with externally bonded fibre-reinforced-plastic plates: design guidelines for shear and flexure. Canadian Journal of Civil Engineering 1998; 25 (4): 692-704.

[19] Zhang L, Subbarayan G. An evaluation of back-propagation neural networks for the optimal design of structural systems: Part I. Training procedures. Comp Method Appl M 2002; 191: 2873-2886.

[20] Zhang L, Subbarayan G. An evaluation of back-propagation neural networks for the optimal design of structural systems: Part II. Numerical evaluation. Comp Method Appl M 2002; 191: 2887-2904.

[21] Sanad A, Saka P. Prediction of ultimate shear strength of reinforced-concrete deep beams using neural networks. J Struct Eng 2001; 127 (7): 818-825.

[22] Levin RI, Lieven NAJ. Dynamic finite element model updating using neural networks. J Sound Vib 1998; 210 (5): 593-607.

[23] Yun CB, Bahng EY. Substructural identification using neural networks. Comput Struct 2000; 77: 41-52.

[24] Zhao Z, Ren L. Failure criterion of concrete under triaxial stresses using neural networks. Comp Aided Civil Infrastruct Eng 2002; 17 (1): 68-73.

[25] Eurocode 2. Design of concrete structures. Part 1: General rules and rules for buildings. BSI Standards, 1992.

[26] Täljsten B, Elfgren L. Strengthening concrete beams for shear using CFRP-materials. Evaluation of different application methods. Compos Part B-Eng 2000; 31(2): 87-96.

[27] Cheng JF, Teng JG. A shear strength model for FRP-strengthened RC beams, Fibre-reinforced Plastics for Reinforced Concrete Structures, Cambridge, UK, Thomas Telford, 2001; 1: 205-214.

[28] Täljsten B. Strengthening of existing concrete structures: design guidelines. Division of Structural Engineering, Lulea University of Technology, Sweden 2003.

[29] Neubauer U, Rostasy FS. Design aspects of concrete structures strengthened with externally bonded CFRP plates, Concrete and Composites. Proceeding of the 7th International Conference on Structural Faults and Repair 1997; 2: 109-118.

[30] Denton SR, Shave JD, Porter AD. Shear strengthening of reinforced concrete structures using FRP composites, Advanced Polymer Composites for Structural Applications in Construction, Eds: Hollaway, Chryssanthopoulos and Moy, Woodhead Publishing Limited 2004: 134-143.

[31] Monti G, Liotta MA. Test and design equations for FRP-strengthening in shear. Constr Build Mater 2007; 21:.799-809

[32] EHE. Instrucción de hormigón structural. Ministry of Public Works 2000 (in spanish).

[33] BS 8110. Structural use of concrete. Part 1: Code of practice for design and construction. British Standard, 1997.

[34] ACI 318-02. Building code requirements for structural concrete. Reported by ACI Committee 318. American Concrete Institute, Farmington Hills, Michigan, USA, 2002.

[35] Garson GD. Interpreting neural-network connection strengths. AI Expert 1991; 6 (4): 47-51.

[36] Kamiharako A, Maruyama K, Takada K, Shimomura T. Evaluation of shear contribution of FRP sheets attached to concrete beams. Proceedings of the III International Symposium Non Metallic (FRP) Reinforcement for Concrete Structures, Japan 1997: 467-474.

[37] Umezu K, Fujita M, Nakai H, Tamaki K. Shear behavior of RC beams with aramid fiber sheet. Proceedings of the III International Symposium Non Metallic (FRP) Reinforcement for Concrete Structures, Japan 1997: 491-498.

[38] Funakawa I, Shimono K, Watanabe T, Asada S, Ushijima S. Experimental study on shear strengthening with continuous fiber reinforcement sheets and methil methacrylate resin. Proceedings of the III International Symposium Non Metallic (FRP) Reinforcement for Concrete Structures, Japan 1997: 475-482.

[39] Tearwe L, Khalil H, Matthys S. Behavior of RC beams strengthened in shear by external CFRP sheets. Proceedings of the III International Symposium Non Metallic (FRP) Reinforcement for Concrete Structures, Japan 1997: 483-490.

[40] Norris T, Saadatmanesh H, Ehsani MR. Shear and flexural strengthening of RC beams with carbon fiber sheets. J Struct Eng 1997; 123(7): 903-911.

[41] Park SY, Namaan AE, Lopez MM, Till RD. Shear strengthening effect of RC beams using glued CFRP sheets, Proceedings of the International Conference on FRP Composites in Civil Engineering, Hong Kong, China 2001; 1: 669-676.

LIST OF FIGURES

LIST OF TABLES

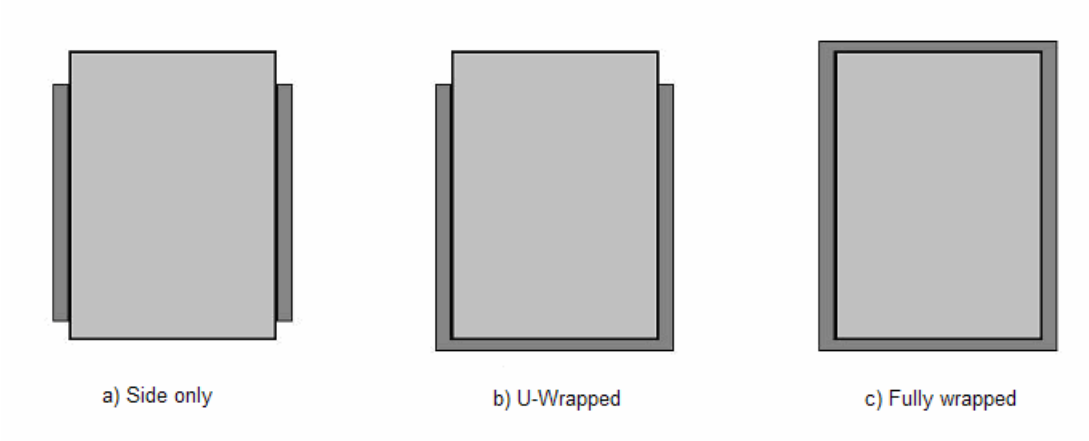

Figure 1. FRP shear strengthening configurations

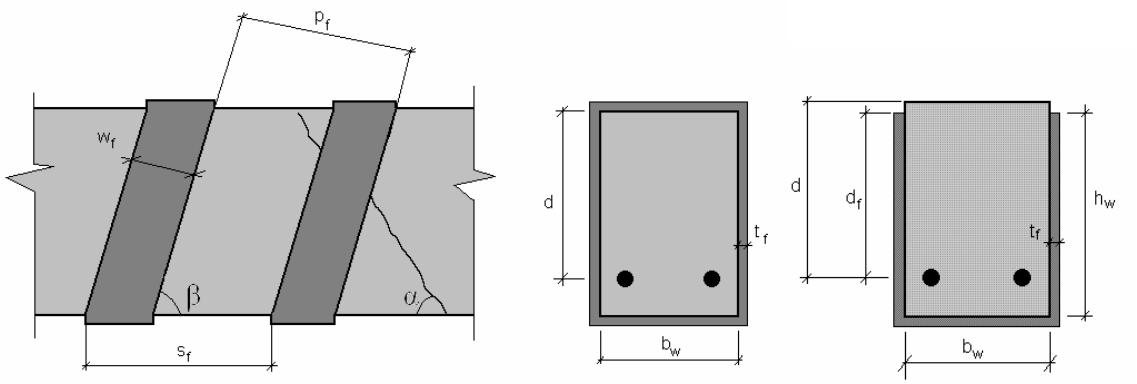

Figure 2. General notation for shear strengthening

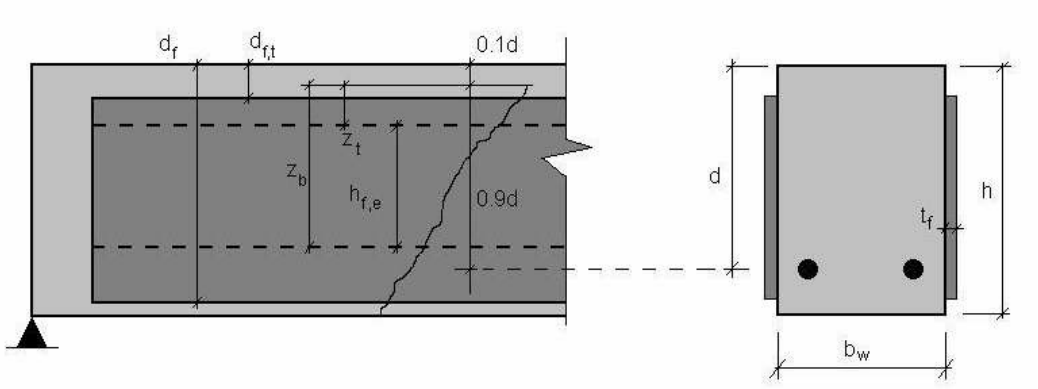

Figure 3. Notation for the Cheng and Teng's model

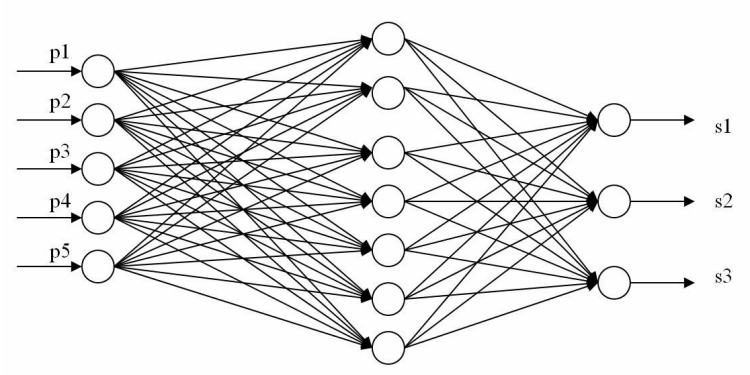

Figure 4. A three layer feedforward neural network

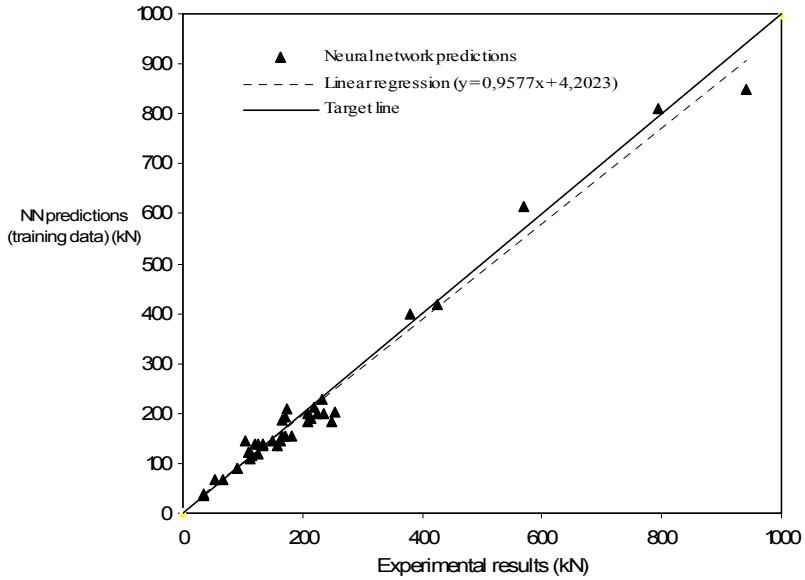

Figure 5a. Comparison of shear strength obtained by the NN model – Training pattern

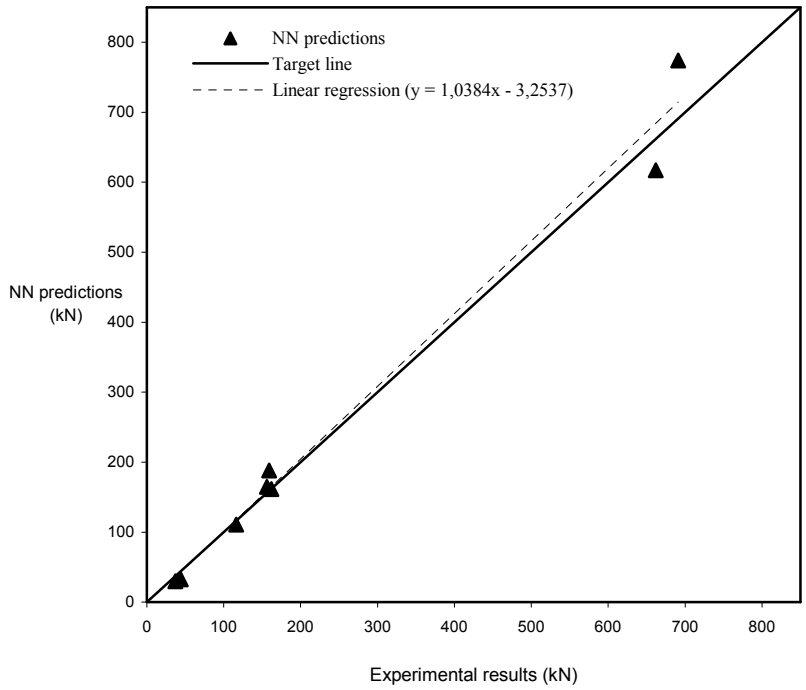

Figure 5b. Comparison of shear strength obtained by the NN model – Validation pattern

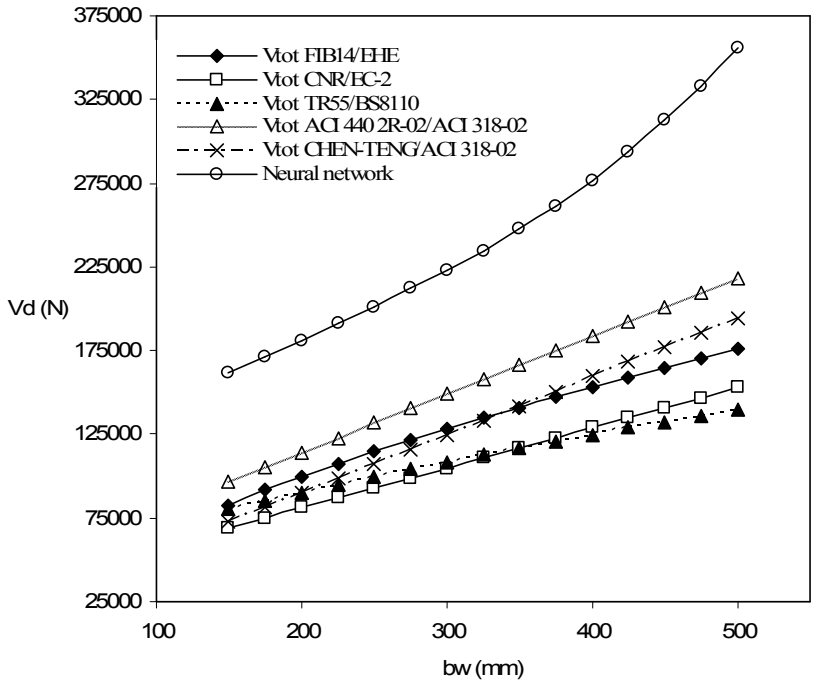

Figure 6a. Beam width effect

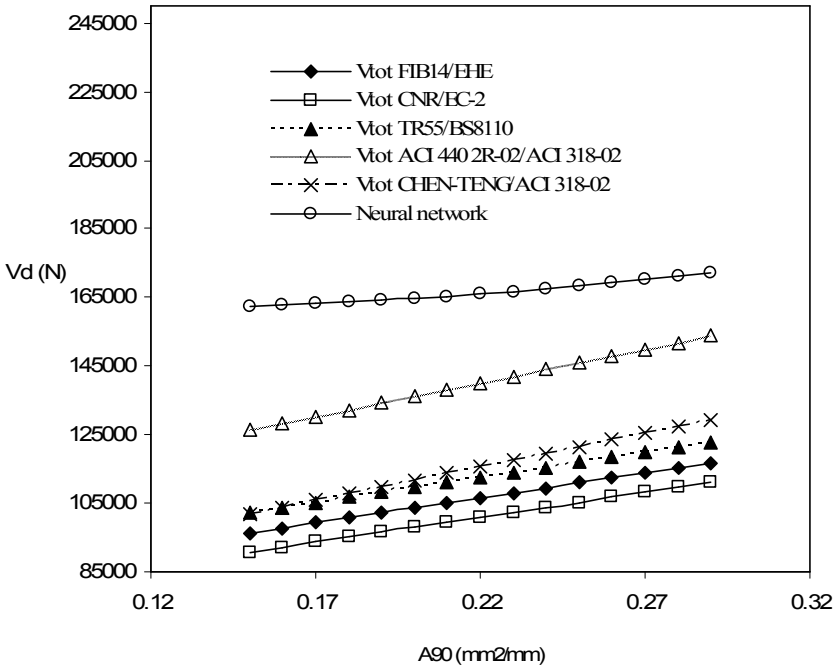

Figure 6b. Effect of the cross sectional area of transverse steel

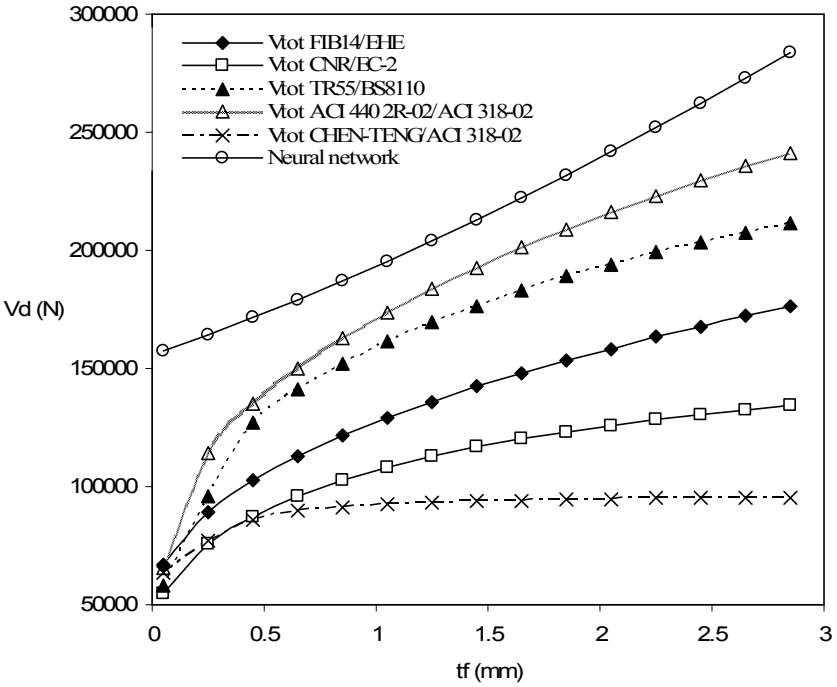

Figure 6c. Effect of the FRP thickness

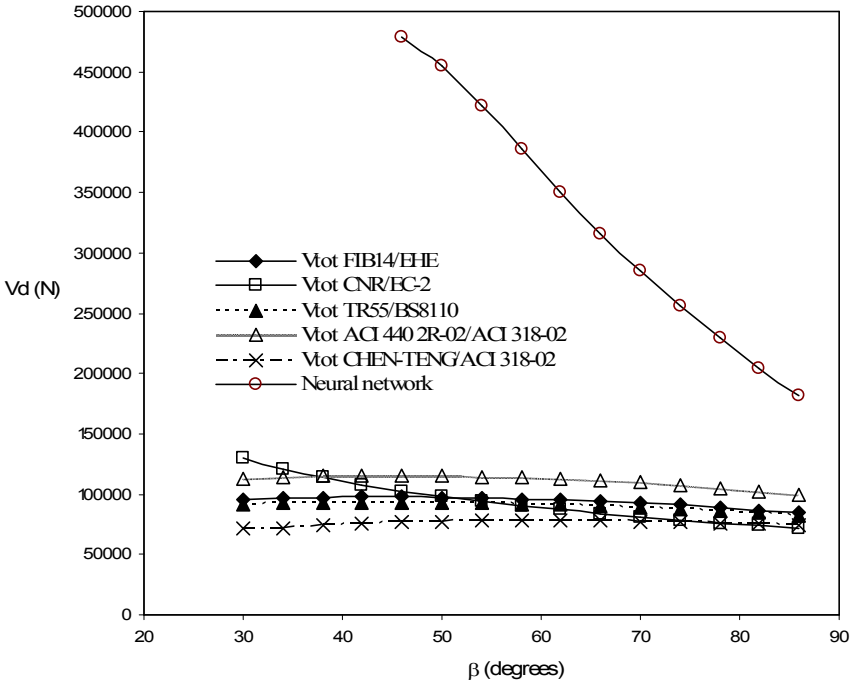

Figure 6d. Effect of the angle between the principal fibre orientation and the longitudinal axis of member

Table 1. Summary of values of mean error for all prediction models

FRP contribution	FIB 14		CNR-DT	TR-55		ACI 440.2R-02	CHEN-TENG	
Concrete and steel stirrups contribution	EC-2	EHE	EC-2	BS 8110	EC-2	ACI 318-02	EC-2	ACI 318-02
Mean error (%)	30,7	27,14	38,9	37,3	47,9	30,8	63,1	48,3
Standard deviation	17,08	23,34	15,31	16,11	14,85	31,99	21,39	19,98

Table 2. Shear strength predictions for the validation pattern (kN)

	BT 2	BT 4	CS 2	CS 3	AB 11	S 2	G	3
Experimental results	156,0	162,0	159,0	116,0	662,0	691,0	37,0	44,0
NN	164,9	161,6	188,1	110,9	617,0	774,0	29,8	32,6
fib 14/EC-2	90,8	73,6	94,2	65,1	527,5	517,2	16,6	33,2
fib 14/ EHE	99,5	82,0	106,8	70,6	547,9	507,9	19,6	39,3
CNR DT/EC2	108,7	69,0	78,6	64,1	349,3	440,3	27,3	24,5
TR 55/ BS 8110	87,5	80,2	83,2	53,5	269,0	445,0	26,6	46,3
TR 55 / EC-2	74,6	67,6	66,7	45,8	224,4	351,1	22,8	36,7
ACI 440.2R-02/ACI 318-02	162,9	96,9	105,7	69,3	361,6	569,6	25,6	47,4
Chen and Teng /EC-2	47,3	56,1	58,1	37,6	207,3	310,2	15,0	15,9
Cheng and Teng /ACI	63,5	72,4	90,4	54,3	288,9	419,1	18,0	20,8

Table 3. Mean errors of NN and design guidelines models

FRP contribution	fib 14		CNR-DT	TR-55		ACI 440.2R-02	Cheng and Teng		NN
Concrete and steel contribution	EC-2	EHE	EC-2	BS 8110	EC-2	ACI 318-02	EC-2	ACI 318-02	
Mean error (%) (Training + Validation pattern)	30,7	27,14	38,9	37,3	47,9	30,8	63,1	48,3	9,98
Mean error (%) Validation	38,3	32,4	42,2	40,5	49,9	27,5	64,2	51,4	11,6

Table 4. Garson index values for the NN input parameters

Parameter	b_w	h	ρ_l	A_{90}	f_{ck}	$f_{y90,d}$	ρ_f	β	E_f
Garson index	0.0718	0.0705	0.1279	0.1441	0.0496	0.1156	0.1604	0.1373	0.1228

Table 5. FRP contribution to the shear capacity

Identification code	Tests (N)	fib14(N)	CNR (N)	TR-55 (N)	ACI (N)	Chen and Teng (N)
US60	13000	72102,9	33714	31548	36242	2907
USVA	22000	67440,0	47769	28252	32455	3781
USV+	37000	67440,0	47769	28252	32455	3781
US45+	27500	64744,6	45294	26653	30618	3639
UF90	27000	78956,2	19832	53273	61198	2620
US45++	35500	62102,7	45087	25113	28849	3496
WS45++	60500	62102,7	65037	35180	87364	16799
US45+ "A"	69000	93413,8	83522	50226	57698	5060
US45++ "B"	74000	93413,8	83522	50226	57698	5060
US45++ "C"	84850	93413,8	83522	50226	57698	5060
US45++ "F"	52150	82307,2	62641	37669	43274	4477
US45++ "E"	65450	82307,2	62641	37669	43274	4477

Table 6. FRP contribution to the shear capacity after the modifications

Identification code	Tests (N)	fib14(N)	fib14/Tests	fib14*(N)	fib14*/Tests
US60	13000	72102,9	5,5	34893,7	2,7
USVA	22000	67440,0	3,1	34578,3	1,6
USV+	37000	67440,0	1,8	34578,3	0,9
US45+	27500	64744,6	2,4	33196,3	1,2
UF90	27000	78956,2	2,9	20166,0	0,7
US45++	35500	62102,7	1,7	31841,7	0,9
WS45++	60500	62102,7	1,0	31841,7	0,5
US45+ "A"	69000	93413,8	1,4	47895,8	0,7
US45++ "B"	74000	93413,8	1,3	47895,8	0,6
US45++ "C"	84850	93413,8	1,1	47895,8	0,6
US45++ "F"	52150	82307,2	1,6	42201,1	0,8
US45++ "E"	65450	82307,2	1,3	42201,1	0,6

fib14*: Eq.(2) with the proposed modifications